ZURICH, SWITZERLAND
6 - 10 OCTOBER 2025

EUROPEAN GEOTHERMAL CONGRESS 2025

# Modelling an ATES geothermal exploitation - From fracture network and aquifer static modelling to hydrothermal simulation of the geothermal doublet

David Polasek[1], Pierre-Clément Damy[1], Marius Gruber[1], Elme Rusillon[1], Aurélien Barrois[2], Patrick Rouvroy[2], Loïc Quiquerez[3].

[1] Hydro-Géo Environnement Sàrl, Geneva, Switzerland

[2] Beicip-Franlab, Rueil-Malmaison, France

[3] Services industriels de Genève, Geneva, Switzerland

david.polasek@hydro-geo.ch

**Keywords:** ATES, geothermal doublet, dual porosity model, discrete fracture network, geological static modelling, hydrothermal simulation.

## ABSTRACT

ATES (Aquifer Thermal Energy Storage) medium-depth geothermal technology uses aquifers to store and extract thermal energy. It allows regulating seasonal temperatures by means of hot and cold wells. This technology principally uses matrix aquifers, due to their good thermal conductivity and ability to effectively store and release heat.

This process is being considered by Services Industriels de Genève (SIG) in the fractured and karstified limestones of the Upper Mesozoic series in the Satigny area (Geneva, Switzerland). By planning a new geothermal doublet, SIG would like to store the residual heat of a heating network in summer and use it in winter. The GEo-01 exploration borehole drilled in 2018, located close to the study area, indicated favorable characteristics for the implementation of such a system, such as high permeabilities and low hydraulic flow.

However, the heterogeneity and complexity of fractured aquifers, as well as the presence of preferential conduits in this geological context can complicate the implementation of this technology. To assess its feasibility, a DFN (Discrete Fracture Network) model was built using offset well data (including GEo-01), 2D seismic data and outcrop analog (Jura mountains) data. This model needed to mitigate hydrogeological uncertainty in the project area by integrating spatial, field, geophysical and well data to assess the equivalent parameters of the dual environment present in the targeted geological formations.

The hydrogeological parameters were dynamically calibrated. An uncertainty analysis was run to determine which of the geological, hydrogeological or operational parameters could have the major influence on the pressure and temperature conditions to be expected, with a view to optimize the energy efficiency of the exploitation. The main outcomes of this analysis are as follows:

- Fracture permeability and production rate essentially control pressure differentials across wells;
- Block size and production rate mainly influence production temperature evolution;
- Sustainable and even enhanced production parameters are found in both wells of the doublet over 30 years, with limited impact on GEo-01.

These promising results allowed the launch of the execution phase of this ATES project. Additional drilling data from the doublet boreholes, as well as the integration of 3D seismic interpretation data in the Satigny area will help updating the simulation of this reversible exploitation and specifying the production parameters required for its sustainable use.

## 1. INTRODUCTION

A geothermal energy development and exploitation project is led by the energy supplier of Canton of Geneva, Switzerland, (Services Industriels de Genève “SIG”), in the frame of the decarbonized energy transition and the Swiss 2050 energy strategy. This national strategy aims at increasing energy efficiency and supporting the development of renewables, including geothermal energy. The national objective of 11.4 TWh of share of renewables in the energy mix is set for 2035 (SFOE, 2018).

The geothermal exploration program of SIG for the Canton of Geneva, GEothermies, was launched in 2012 and is still ongoing. Two geothermal exploration wells were drilled in 2018 and 2020 (GEo-01 and GEo-02, respectively), and a 187 km² 3D seismic survey was shot in 2021. GEo-01 identified exploitable hydrothermal resources in the fractured limestones of the Upper Mesozoic series, in the Satigny area.

An ATES (Aquifer Thermal Energy Storage) medium-depth geothermal system is considered by SIG to produce these identified resources. This technology allows regulating seasonal temperatures of surface infrastructures by storing excessive heat in summer and producing it in winter. ATES systems are built similarly to a geothermal doublet, but with an asymmetrical geometry, with a shallower cold well and a deeper hot well, each connected to different, loosely connected aquifers. ATES systems principally uses matrix aquifers, due to their good thermal conductivity and ability to effectively store and release heat. They are sensitive to hydrogeological conditions and they must avoid high hydraulic flow and mineralized fluids (Fleuchaus et al., 2018).

Despite being set in fractured, karst and carbonate aquifers, the hydraulic tests of GEo-01, as well as several hydrogeological studies, indicated good potential for an ATES exploitation in Satigny: high permeability, low hydraulic flow and low-dissolved-element content.

An ATES modelling study was carried out in the Satigny area, close to the geothermal well Geo-01 (figure 1). An innovant and specific approach was followed in order to characterize the complexity of the fractured aquifers, using various type of existing data to lower uncertainties and optimize the operational parameters and the exploitation design.

## 2. GEOLOGICAL SETTINGS

The Satigny area is located in the Western Swiss Molasse Basin (WSMB), which was formed by lithospheric flexion during the Cenozoic Alpine orogenesis. It is bounded in the SE by the outer Alps and in the NW by the Jura fold-and-thrust belt (figure 1). The sedimentary cover, made of a thick Mesozoic carbonate sequence, was detached from the hercynian, metamorphized basement by the distant push of the Alpine collision over decollement layers in the Muschelkalk and Keuper evaporites (Buxtorf, 1907; Affolter et al. 2008).

Results of geological studies and analysis in the Geneva Basin gathered precious information on local stratigraphy and its lateral variability (Rusillon 2017; Brentini, 2018, HGE, 2021a; 2021b; 2023a; 2023b). The carbonate sequence of the Mesozoic comprises isostasic fluctuations and several regression and transgression cycles, recorded by carbonate sedimentology. These cycles are reflected in the WSMB by heterogeneous depositional environments presenting alternating limestone and marls units,

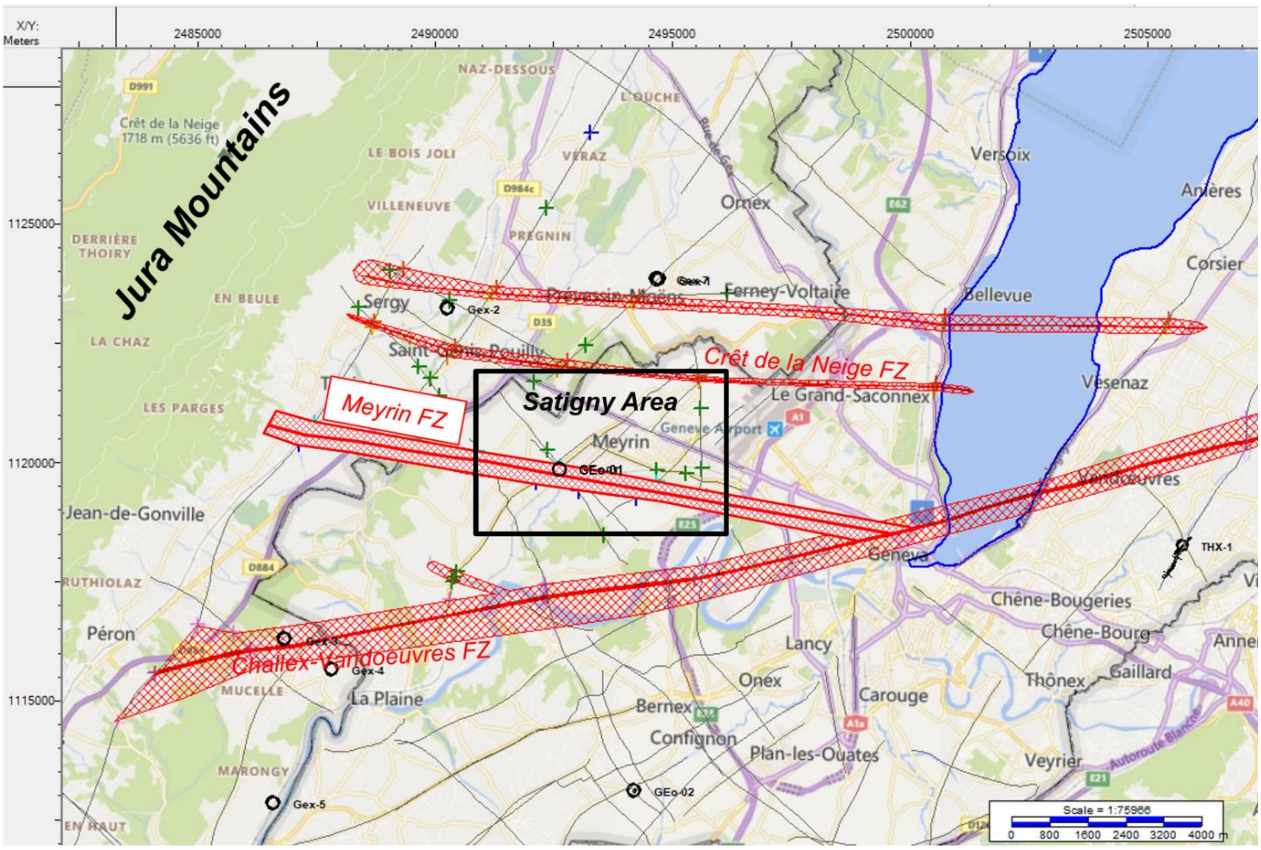


**Figure 1: Location of the study area (Satigny), offset wells, particularly GEo-01, 2D seismic survey and large structural framework applied for modelling.**

occasionally affected by secondary dolomitization (figure 2).

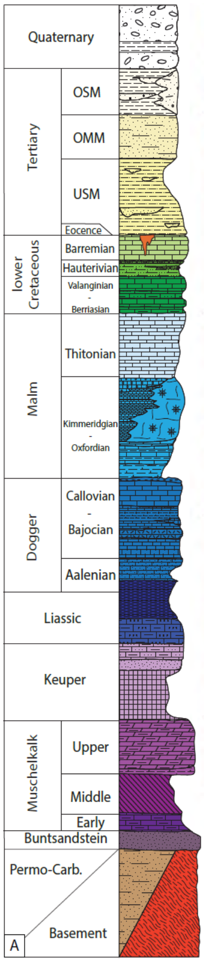


**Figure 2 : Stratigraphical column of the Satigny area (modified after Rusillon, 2017)**

Recent Cenozoic tectonic activity has greatly contributed to the present structural situation of the Molasse Basin. An initial period of N-S compression at the beginning of the Eocene, responsible for the Pyrenean orogeny, affected the area through combined NW-SE and NE-SW strike-slip faults. During the Oligocene, flexure of the foreland led to the formation of NE-SW trending extensional faults, partially reactivating the Eocene faults. In the early Miocene, strong NW-SE lithospheric compression led to the formation of the Jura Fold-and-Thrust belt to the NW of the WSMB. In this tectonic context, numerous strike-slip faults also developed in the Jura and Molasse basin, giving rise to the present structural context observed in Satigny. These subvertical faults have a combined WNW-ESE and NNW-SSE geometry, with some variations due to local rotations of the stress field, as well as the reactivation of inherited structures (Clerc & Moscariello, 2020; Polasek, 2020; Schori, 2021; Hauvette, 2023).

### 2.1 Aquifers

Geothermal exploration in the Geneva Basin is focused on fractured and karst potential aquifers. Only local, diagenetically-constrained well-developed matrix aquifer properties have been identified in the Mesozoic sequence. Despite coarse bioclastic facies observation in several intervals of the Geneva Basin stratigraphic column, complex diagenesis has jeopardized efficient fluid circulation in undeformed formations, except for karst development bound to inception horizons (HGE, 2023a). Thus, geothermal targets constitute fault zones or fracture corridors where reservoir properties may be enhanced by open and active fracture network development.

As aquifer properties and quality mainly rest on the presence of secondary permeability structures, a significant emphasis has been placed on structural characterization of the Satigny area. A Discrete Fracture Network (DFN) model was needed to mitigate hydrogeological uncertainties and thus assess the equivalent parameters of the dual environment present in the targeted geological formations of the Cretaceous, Malm and Dogger. Lateral and vertical variability was studied for rendering accurate aquifer properties, which could only be depicted by a detailed static model in order to simulate effective exploitation.

### 2.2 Hydrogeological concepts

Based on previous geothermal reservoir characterization (HGE, 2021a), flows and heat transfers in the Geneva basin have been modelled (HGE 2023b). This made possible to constrain and understand the parameters influencing the distribution of temperatures and hydraulic loads, and to characterise the link between the recharge zone on the Jura Mountains and the Geneva basin. Key identified concepts are:

- A quasi-impermeable hydraulic barrier corresponding to the backthrust of the Jura, which buffers the hydraulic link between the Jura and the basin;
- Compartmentalization of hydraulic potential in the basin, controlled by major fault systems;
- Less permeable thrust systems, as observed and indicated by the hydraulic tests of GEo-02 and Thônex-1;
- Enclosing formations with high hydraulic conductivities, as observed from very rapid stabilisation of the drawdown and re-pressurisation of GEo-01 during its long-term tests;
- Significant hydraulic conductivity anisotropy along fault zones as inferred by the long-term tests of GEo-01 and the water residence times estimated by geochemical methods;
- The presence of high hydraulic potentials along fault zones in the North of the Basin, providing a large quantity of water to replenish the basin, particularly observed during the long- term tests of GEo-01;
- Increased heat flows in the vicinity of strike-slip faults as inferred from high geothermal gradients observed and synonymous with convection cells.

## 3 FRACTURE NETWORK MODELLING

Static modelling was conducted from geological, structural, geophysical, geomechanical and hydrogeological data available for the Satigny area and its surroundings. The model area was defined around the Meyrin fault zone, with a surface of approximately 6,500 x 4,000 m, needed to effectively simulate fluid flow. A 2D seismic interpretation of the Satigny area was realized with the Kingdom suite from vintage seismic profiles, with the following horizons: Top Cenozoic, Top Cretaceous, Top Upper Malm, Top Lower Malm, Top Dogger, Top Liassic, Top Triassic. The principal fault plane of the Meyrin fault zone was interpreted, along with lateral limits of its damage zone (seismic degraded zones; figure 3). A 3D seismic survey was conducted in 2021 in the whole Geneva region, but its results weren't available in time for this study.

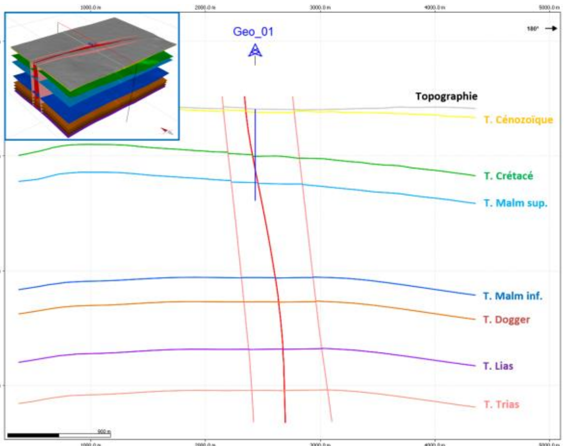


**Figure 3 : 3D model of the Satigny area, based on 2D seismic interpretation. GEo-01 is projected on the section.**

A 3D pillar grid was generated from the 3D surface geological model with Petrel. The vertical extent of the grid was limited from surface topography to Top Keuper, as the above-laying marly and shaly Liassic units are considered as a regional seal, with very limited to absent hydraulic connectivity through it.

Fracture modelling and equivalent parameters computation were realised with Fracaflow. Several steps are needed to build a static model (figure 4): Static well data analysis, static inter-well data analysis (seismic and analogue data), dynamic analysis (well tests and flowmeter data), fault and fracture network conceptualisation, fault and fracture modelling with a Discrete Fracture Network (DFN), DFN dynamic calibration, and equivalent parameters computation (upscaling).

### 3.1 Fracture and fault analysis

GEo-01 static and petrophysical data was collected and analyzed regarding the observed fracture network that was crossed by the well. Several image log interpretations were made from different authors (HGE, 2019; Koumrouyan, 2019; Lo, 2019). Comparisons between these works were conducted, leading to the selection of one dip interpretation for implementation in the Satigny modelling workflow. Criteria such as dip plane amount, dip type differentiation (fractures, stratigraphic boundaries, etc.) and interpretation similarity between authors led the selection. The dip interpretation of Koumrouyan (2019) was selected, and this fracture interpretation was differentiated between fracture sets, which resulted in 3 main ones: NNW-SSE, W-E and NE-SW-striking fractures with oblique dip angles (N080/15, N355/35 and N131/49 dip azimuth and dip, respectively). GEo-01 being vertical, dip angles observed on its image logs are biased and not necessarily representative of those of the fracture network surrounding it (Terzaghi, 1965; Sanderson & Nixon, 2015). However, dip variability was considered int the DFN model. Fracture density along GEo-01 was then calculated over the imaged portion of the well. P10 densities (Dershowitz and Herda, 1992; Sanderson & Nixon, 2015) were calculated every 2m, over an 8m sampling window. Densities per family ranged from 0 to around 5 frac/m. At several points in the well, frac clusters are present, with contributions from all frac families, bringing the maximum density to 9.4 /m. Fracture criticality based on stress analysis was computed to assess the mechanical and hydrogeological activity of the fracture sets (Townend & Zoback, 2000; Ferrill et al., 2020). Stress parameters based on regional compilation (HGE, 2022) was adapted on the local scale of the Meyrin fault zone and its probable impact on stress perturbation and reorientation. The stress analysis results were used for dynamic calibration of the DFN model (cf. chapter 3.5).

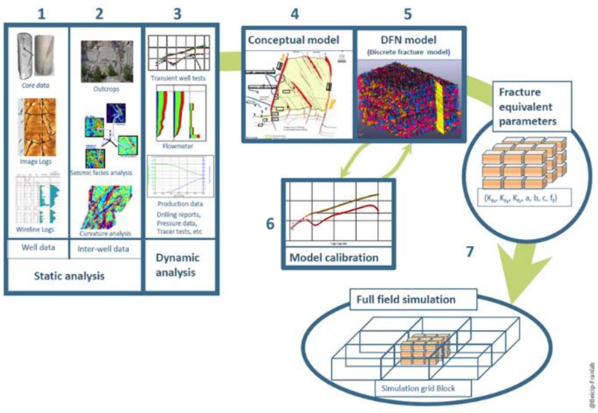


**Figure 4: Static model creation, from data analysis, model conceptualisation, DFN modelling and calibration, and equivalent parameters computation (from Beicip-Franlab, Fracaflow documentation).**

Inter-well data analysis is needed to conceptualize the fault and fracture network expected in the model area, aside from well observations. Seismic data, and fault plane interpretations consist in the main inter-well known structures. Fault and fracture networks can be modelled by reproducing seismic-derived fault properties on smaller scale (stochastic sub-seismic fault generation). In the present study, the reproduction of sub-seismic faults has not been integrated, for two reasons: (1) the unique use of fractures of various sets, orientations and densities allows controlled parameterization of their attributes in order to define a realistic preferential flow framework consistent with the hydrogeological observations of GEo-01. This facilitates dynamic model calibration. (2) Given the limited dimension of the modeling block, the presence of a single deterministic fault does not allow sufficient statistical sampling to reproduce stochastic faults of reduced dimensions. The limited amount of data available therefore calls for the most straightforward structural conceptualization, in order to preserve the consistency of the final model.

The Meyrin fault plane was used as the deterministic fault for subsequent modelling. Its mean orientation and dip were analyzed and the attributes of fault distance and P32 fault density (surface/volume) were calculated and imputed to the cells of the 3D mesh model.

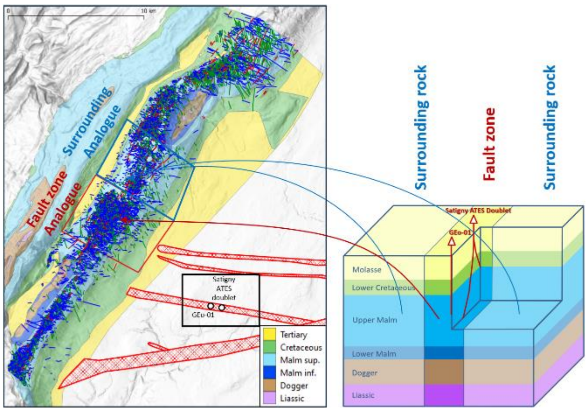


**Figure 5 : Transposition of the morpho-tectonic lineament interpretation of the Jura Moutains innermost anticline in the Upper Malm unit (Polasek, 2020) to the Satigny perimeter for the same unit.**

For completing inter-well structures, fracture networks were analyzed on outcrop analogue in the Jura Mountains. Their deformation kinematics were studied in detail by Polasek (2020) on the innermost anticline. The fracture network was characterized both on outcrops and using digital elevation models, with a morpho-tectonic lineament analysis. Subvertical, WNW-ESE-striking faults similar to the Meyrin fault are present on this first fold. The lineament interpretation carried out was sectioned into a damage zone compartment (fault zone) and a undamaged compartment (surrounding rock) in the outcropping area of the Upper Malm, and was thus used as an analogue to the Satigny modeling perimeter in the same unit (Figure 5). The choice to extrapolate this fracture network only for the Upper Malm unit is dictated by its very extensive outcropping area, allowing a high degree of representativeness and confidence in the use of its statistical properties.

Statistical analysis of the fault zone and surrounding rock lineament network rendered three main fracture sets for both environments, with few statistical differences (figure 6). For conciseness purposes, only modelled fracture network statistics are presented herein (figure 8 and table 1).

### 3.2 Dynamic analysis

Dynamic well data analysis identifies productive and open fractures, targeting in-well water inflows and mud loss intervals, as well as analyzing flowmeter, well test and production data. In the case of GEo-01, the productive intervals were identified during drilling, by their contribution to the observed artesian flow. During the production tests carried out on GEo-01, a change in the productivity index (PI) was observed. By ignoring head losses associated with obstructions or the presence of pipes in the well (for tests during drilling), PI was estimated between 7.5 L/s/bar and 10 L/s/bar, i.e. an estimated artesian flow rate between 75 and 100 L/s.

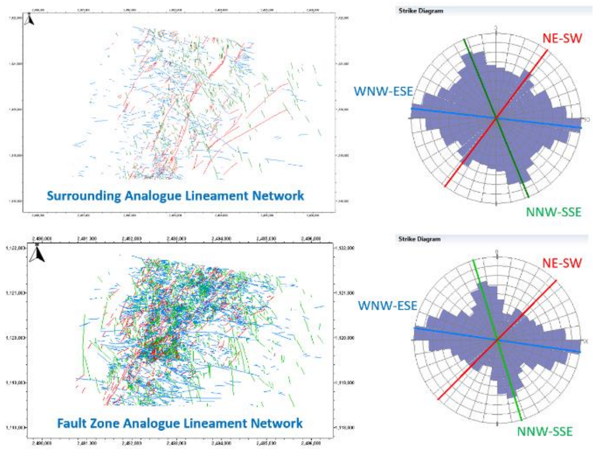


**Figure 6 : Lineament interpretations transposed to the surrounding block and fault zone of the Meyrin-Satigny perimeter. Left: Plan view of lineament interpretations, displayed by families. Right: Lineament orientations plotted on rose diagrams.**

### 3.3 Fracture network conceptualization and fracture density computation

As well data were not available for the complete range of depths, and thus stratigraphic units, of the Satigny volume, and because of the lack of inter-well structural data (no 3D seismic), the conceptualization of the fracture network needed other approaches to depict expected structural conditions in Satigny.

Fracture sets were considered to be the same throughout the stratigraphic column, as their orientation seem to be controlled by the proximity of fault networks that are consistent regionally (Polasek, 2020). Fracture network variability is therefore assumed to vary in density and aperture, which are key parameters for fracture connectivity. Both parameters were addressed by geomechanical issues: Fracture density was estimated with an innovant methodology, which assesses expected density in function of rheology, and particularly the present-day geomechanical conditions of the stratigraphic units. Fracture aperture was estimated from slip and dilation tendency of the fracture set regarding Satigny's expected stress field conditions.

A collection of WSMB offset well geomechanical data has been conducted by HGE (2023c), and this data set was utilized in the present study for deriving a mechanical stratigraphy chart of Satigny's rock units based on their brittleness index (figure 7). Prediction of brittle versus ductile behavior of the stratigraphic units was determined by elastic moduli computation and analysis (Rickman et al., 2008 ; Zhang et al., 2016). Fracture density for every unit and compartment was calculated by extrapolating observed density of the Jura Mountains' lineament network with brittleness of the stratigraphic units, for both tectonic compartments (fault zone vs surrounding rock), and the results were calibrated with GEo-01 structural data. This methodology obviously considers recent fracture initiation, propagation or/and reactivation, and omits fracture networks generated under different tectonic and diagenetic conditions. Yet, as geothermal exploration focuses on fractures being currently mechanically and hydrogeologically active, this approach was used with confidence. Furthermore, geomechanical characterization is also used in this industry for determining geothermal targets with high expected fracture density and connectivity.

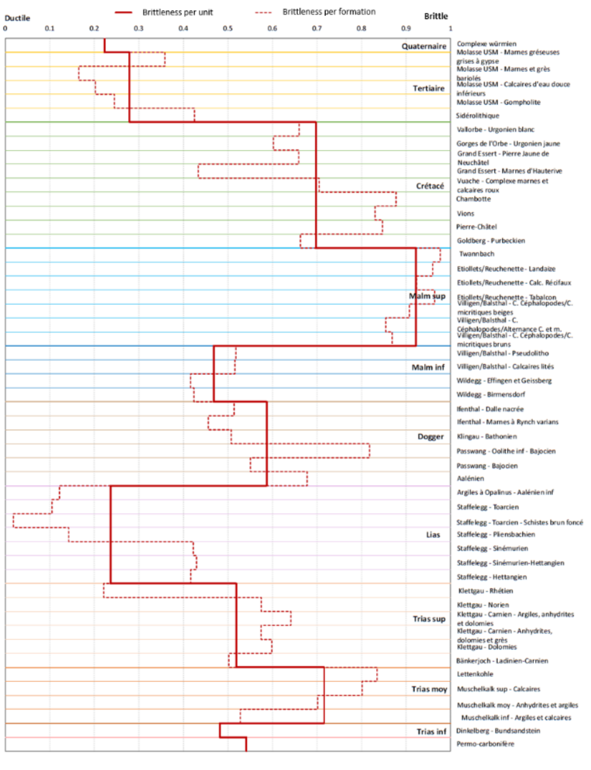


**Figure 7 : Brittleness index of the WSMB stratigraphic units based on offset well data. Average values were calculated per formation and unit. Modified from HGE (2023c).**

Fracture density can evolve in many ways in a fault zone, depending on the configuration of faults and fractures within the zone and the presence of cataclasites forming impermeable gouges in the fault core(s). The proportions between fault core and damage zone are decisive for the evolution of the permeability of the entire zone (Caine et al., 1996; Bense et al., 2013). For static modelling, two fracture density evolution scenarios were considered in the fault zone: The first scenario imitated a distributed conduit, with relatively low importance of gouges in potential fault planes, which induces homogeneous densities and permeabilities throughout the damage zone, with variations by units. This scenario enables the simplest, uncomplicated modeling of equivalent hydraulic parameters from static properties. The second scenario mimicked a relatively localized conduit, involving a gradual increase in densities and permeabilities within the damage zone, with a maximum on the fault plane. The presence of the fault gouge was initially ignored, but could be added if needed during dynamic modelling. After being tested by a sensitivity analysis, the first scenario (distributed conduits, homogeneous properties in the fault zone) was finally chosen for the ATES simulation.

### 3.4 Fracture and fault modeling

After having completed the data analysis, fracture model conceptualization and fracture density computation steps, the DFN was modelled. The Meyrin principal fault plane was reproduced without change in the model as a deterministic fault, and the fracture network was modeled from the set properties, varying for each unit. Orientation, size (length and width) and density parameters were defined according to the previous steps, while indications of fracture openings and conductivities were first approximated during this modelling phase, but verified during dynamic model calibration (chapter 3.5). The final fracture set parameters are summarized in Table 1. The NNW-SSE and WNW-ESE fracture sets are derived from the subvertical and conjugate strike-slip faults present in the WSMB and the Jura Mountains. Their mean dips are therefore also considered as subvertical, and their size distribution was defined on the basis of observations of the analogous fracture network. The NE-SW family refers to thrust and backthrust faults (SE and NW dip azimuth, respectively), as well as extensional fractures that form near fold hinges of various sizes. The folds observed in the basin and on the Jura Mountains have the same NE-SW axial trace orientation, and are observed at different scales, from 1st order folds to intra-formation folding. Dip variability of this fracture set is thus considerable, and all possible dips were represented (Von-mises distribution coefficient of 1). Furthermore, the lateral persistence of these fractures can approach large dimensions, when they are related to thrust faults (max. length: 1'000 m). Orientation distribution of the three fracture sets are presented on figure 8.

**Table 1 : DFN parameters for every fracture set considered. The final aperture and conductivities were defined during dynamic model calibration (chapter 3.5).**

| Fracture set | | NNW-SSE | WNW-ESE | NE-SE |
|---|---|---|---|---|
| Orientation | Mean Azimuth | 073° | 008° | 135° |
| | Mean Dip | 90° | 90° | 90° |
| | Distribution Law | Von-mises | Von-mises | Von-mises |
| | Azimuth Deviation | 0.3 | 0.3 | 0.3 |
| | Dip Deviation | 0.3 | 0.3 | 1 |
| Size | Distribution Law | Power Law | Power Law | Power Law |
| | Mean Length | 16 m | 33 m | 20 m |
| | Min Length | 1 m | 10 m | 1 m |
| | Max Length | 370 m | 365 m | 1000 m |
| | Aspect ratio (length x width) | 0.5 | 0.5 | 0.5 |
| Spatial Distribution | Fracture Density | Calculated Density | Calculated Density | Calculated Density |
| Aperture | Distribution Law | Constant | Constant | Constant |
| | Aperture | 0.455 mm | 0.812 mm | 0.081 mm |
| Conductivity | Law Type | Poiseuille Law | Poiseuille Law | Poiseuille Law |
| | Lambda Parameter | 1 | 1 | 1 |
| | Conductivity | 7 947 mD m | 45 250 mD m | 45 mD m |

### 3.5 Dynamic calibration

The dynamic calibration of the model involves the fracture modeling parameters, which have an impact on the overall conductivity of the aquifer. First, the results of the dynamic analysis were used to estimate the general transmissivity of the reservoir. Then reservoir transmissivity was used alongside the cumulative height of the productive intervals and the drained reservoir zone and radius as a basis for calibrating the hydraulic properties of the DFN. These were optimized by configuring fracture aperture, whose relationships were determined according to the average dilation tendency for the given stress model (table 2). The parameterization coefficient of the NE-SW set was reduced for the following reasons: The mean dip of this set was maintained at 90° during modelling, whereas it should probably display a bimodal distribution of 30-45° dip to the NW and SE due to its association with low-angle thrusting and dip-slip detachment structures.

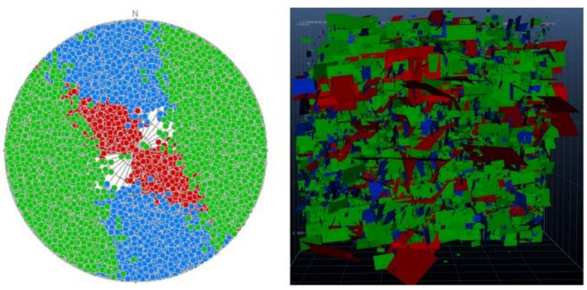

**Figure 8 : Southern hemisphere stereographic projection and graphic representation of the modelled fracture network. The defined fracture families are represented by color: NNW-SSE (green), WNW-ESE (blue) and NE-SW (red).**

### 3.6 Analytical upscaling

The final step in static modeling consisted in calculating the equivalent parameters of the DFN in the modeling grid (analytical upscaling). A wide range of parameters were calculated during this phase, including three-axial fracture porosity, permeability and block size. This final step concluded the static modelling of the Satigny area and presented the geological and structural framework in which fluid flow simulation were realized.

## 4. THERMO-HYDRAULIC MODEL

ATES exploitation simulation was conducted with Pumaflow (simulation) and Cougarflow (sensitivity analysis) on the static model to verify and optimize the operational parameters that would make the exploitation viable. As fractured aquifers present complex characterization issues, the focus was put on a number of geological parameters linked to fractured media that could complicate a ATES exploitation, such as: (1) the presence of preferential conduits, which can lead to uneven distribution of heat and/or cold and thus greatly reduce the efficiency of the thermal storage, (2) the presence or absence of a hydraulic flow, which can lead to significant dilution of the stored heat or cold.

**Table 2 : Calibration of fracture aperture and parameter relationships between sets.**

| Fracture Set | NNW-SSE | WNW-ESE | NE-SE |
|---|---|---|---|
| Identifier | A | B | C |
| Mean Dilation Tendency | 0.56 | 1 | 0.5 |
| Parameterization | 0.56 * B | B | 0.1 * B |
| Calibrated Aperture | 0.455 mm | 0.812 mm | 0.081 mm |

With the aim of using a virtuous cycle to produce warm water in winter and cool water in summer, and to assess possible hydraulic and thermal interference between the 3 wells, a numerical modelling combined with uncertainty analyses on uncertain parameters were carried out. The geothermal doublet planned by SIG will comprise two wells at different depths: Satigny-2 will have an open section in the Lower Malm formation, and Satigny-3 will have a section open in the Upper Cretaceous and Upper Malm. SIG envisages Injection at 15°C into the cold well (Satigny-3) from October 27 to April 10 (winter period), and injection at 69°C into the hot well (Satigny 2) from May 20 to September 17. A constant production is considered for GEo-01 (figure 9).

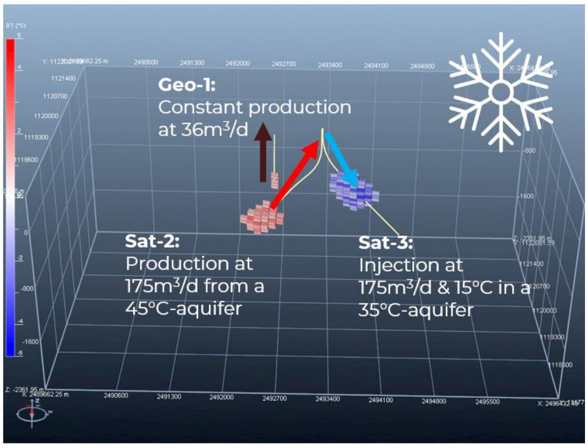


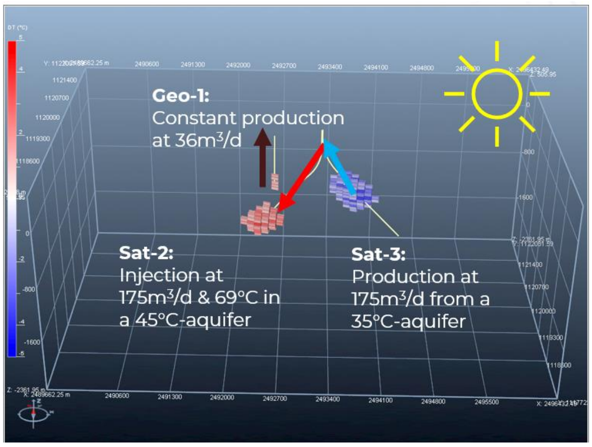


**Figure 9: Schematic diagrams of the reversible operation of the Satigny geothermal doublet depending on seasons. Above: Winter exploitation. Below: Summer exploitation.**

### 4.1 Initial state

From a thermal point of view, a variable gradient was imposed on the reservoir to represent the temperature distribution in the reservoir. This geothermal gradient is derived from the temperature data observed on GEo-01 and interpreted according to the various temperature data measured on the molasse basin:

- 10°C at the surface
- 33.8°C at 650 m - Gradient of 3.7 °C /100
- 60.1°C at 2000 m - Gradient of 2° C/ 100 m
- 90.8°C at 3000 m - Gradient of 3° C/ 100 m

The pressure observed at GEo-01, i.e. 84 bar at a depth of 744 m, was used as the reference pressure for the reservoirs modelled. The pressure gradient is then calculated using the PVT (Pressure, Volume, Temperature) used in the modelling. A total dissolved solids (TDS) concentration of 1 g/l was imposed on the entire reservoir. To simulate variations in fluid viscosity and density with pressure, temperature and dissolved solids, the internal equations integrated into Pumaflow (PVT) were used.

### 4.2 Exploitation simulation and uncertainty analysis

Simulations were realised for a 30 year geothermal exploitation period. Monte-Carlo analyses were conducted for presenting a complete panorama of outcomes as well as their related uncertainties. The uncertainties of the following geological, hydrogeological and operational parameters were considered:

- Block size (or fracturing density);
- Fracture permeability;
- Matrix permeability;
- Heat capacity by volume of the solid;
- Thermal conductivity of the solid;
- Regional hydrogeological flows between the Jura and a potential outlet to the east (referred to here as hydrothermal flows);
- Variation in GEo-01 flow rates;
- Variation in Satigny doublet flow rate.

The uncertainty analysis led to a ranking of parameters in function of their importance on pressure and temperature results was realized for each well (Satigny-2, Satigny-3 and GEo-01). The results of Monte-Carlo simulations were synthesized in 3 scenarios: P10, P50 and P90 (table 3). Several key elements for understanding the Satigny doublet and GEo-01 geothermal exploitation came out of the analysis:

- The pressure differentials across the wells are essentially a function of the fracture permeability of the medium and the production rate of the well;
- Because of the very high fracture permeability of the reservoir under consideration, the pressure differentials modelled for all the scenarios are less than 5 bar for P90.
- Block size and well production rate are the major controlling parameters for Satigny-2, Satigny-3 and GEo-01 production temperature evolution over 30 years of operation. The smaller the block size (i.e. the more diffuse the fractured medium), the more efficient the storage, and the higher the production temperature for Satigny-2 and the lower for Satigny-3.

More specifically, for each well:

- Satigny 2: Production temperature after 30 years of operation would be 60°C for P10 and 52°C for P90 instead of the initial 45°C (figure 10).

**Table 3 : Synthesis of Monte-Carlo analysis results for pressure and temperature in scenarios P10, P50 and P90, for a 30 year exploitation simulation of the Satigny geothermal doublet and GEo-01.**

| Parameters | Scenario | Satigny-2 | Satigny-3 | GEo-01 |
|---|---|---|---|---|
| Pressure differential over 30 years of operation | P10 | < 1 bar | < 1 bar | P10 : < 1 bar |
| | P50 | < 1 bar | ≈ 2 bar | P50 : < 1 bar |
| | P90 | ≈ 2 bars | ≈ 5 bars | P90 : ≈ 4 bars |
| | Major controlling parameter | Fracture permeability + Satigny flow rate | Fracture permeability + Satigny flow rate | Fracture permeability + GEo-01 flow rate |
| Production temperature after 30 years of operation | P10 | ↗ 15°C | ↘ 20 °C | P10 : ↗ 3.5 °C |
| | P50 | ↗ 12°C | ↘ 16 °C | P50 : ↗2.5 °C |
| | P90 | ↗ 7°C | ↘ 10 °C | P90 : ↗ 1.5°C |
| | Major controlling parameter | Bloc size (fracture density) + Satigny flow rate | Bloc size (fracture density) | GEo-01 flow rate |

- Satigny 3: Production temperature after 30 years of operation would be 18°C for P10 and 28°C for P90 instead of the initial 38°C
- GEo-01: Production temperature after 30 years of operation would increase by 3.5°C for P10 and 1.5°C for P90.

## 5. DISCUSSION

Geothermal potential was confirmed in Satigny area by the results of a first exploration well realized by SIG on the trace of the Meyrin fault zone. An ATES doublet is considered for optimal geothermal exploitation in this fractured aquifer that showed persuasive hydraulic properties. However, fracture network characterization and modelling represents a considerable challenge in this context: only one well was drilled in the zone, without crossing the complete stratigraphic series and geological targets. Additionally, no 3D seismic surveys were shot in the area at the time of the study. The present study proposes an innovant methodology based on the described case study for characterizing the expected fracture network by linking reliable structural and geomechanical analyses of different scales and combining them in a concordant area of interest.

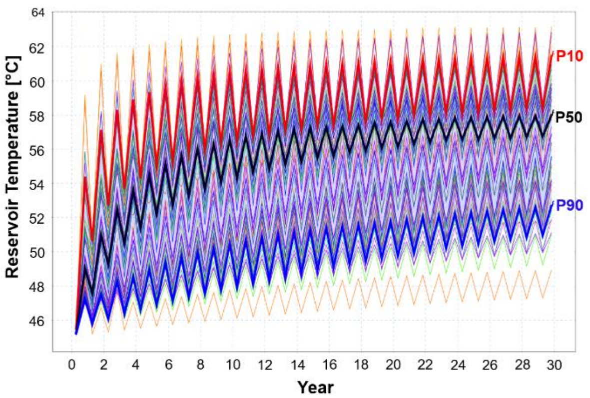


**Figure 10: Satigny-2 temperature trends over 30 years of operation for all the simulations carried out (in red P10, in black P50 and in blue P90)**

In the Satigny case, the neighboring Jura Mountains display outcrops of the Upper Mesozoic carbonates, which dip in the WSMB at favorable depth range and constitute the aquifer targeted by geothermal exploration programs. Multi-scale extended structural analyses made on this outcropping units are considered consistent and appropriate for comparisons in the basin. Fault zones and fracture networks show similar sets and structural properties, and thus they constitute a valuable analogue to basin exploration. Geomechanical findings made in the WSMB were ideal for implementing them in the process and complementing structural and hydrological characterization of the Satigny area by predicting fracture occurrences based on rheology and current stress state.

Several additional studies would be beneficial for optimizing the Satigny ATES plant operational parameters, especially the doublet static and dynamic data, and long-term hydraulic tests that could be conducted between GEo-01, Satigny-2 and Satigny-3. Tracer tests between these wells could add valuable information on the hydraulic situation of the Meyrin fault. 3D seismic data, from a survey that was shot in the Geneva region, and processed and interpretated during the realization of the present study, should be added to static modelling for precising fault geometry, occurrence, orientation, density and kinematics. The resulting static model and dynamic simulations would be even more robust with these additions.

## 6. CONCLUSION

An ATES exploitation is considered in Satigny, Geneva, by SIG in the Meyrin fault zone. GEo-01, the first well of the SIG geothermal exploration program showed convincing structural and hydraulic properties in the aquifers tapped in Satigny.

Structural analysis, and especially fracture network modelling, needed to account for the complexity of the fault zone, in order to provide reliable hydraulic properties for simulating the ATES exploitation over a 30 year timespan. An innovant methodology is proposed in this case study to complement available data with multi-scale analogue observations and to integrate geological, structural, hydrogeological and geomechanical information in reliable concepts linking static and dynamic models. Monte-Carlo analyses of the dynamic simulations showed the importance of structural and operational parameters in the ATES exploitation viability. Probabilistic results and scenarios displayed promising, and even enhanced reservoir exploitation conditions after the 30 year period with the ATES doublet. These results should be complemented with the doublet and 3D seismic data for optimal characterization of the Satigny area.

**REFERENCES**

Affolter, T., Faure, J.-L., Gratier, J.-P., Colletta, B.: Kinematic models of deformation at the front of the Alps: new data from map-view restoration, *Swiss Journal of Geosciences*, **101**, (2008), 289–303.

Bense, V.F., Gleeson, T., Loveless, S.E., Bour, O., Scibek, J.: Fault zone hydrogeology. *Earth-Science Reviews,* **127**, (2013), 171–192.

Brentini, M. : Impact d'une donnée géologique hétérogène dans la gestion des géo-ressources: analyse intégrée et valorisation de la stratigraphie à travers le bassin genevois), Thèse de doctorat, *Université de Genève*, Geneva, (2018), 236p.

Buxtorf, A.: Zur Tektonik des Kettenjura : Berichte über die Versammlungen des Oberrheinischen Geologischen Vereins, *Ber. Versamml. Oberrhein. Geol. Ver.*, Lindau, (1907).

Caine, J.S., Evans, J.P., Forster, C.B.: Fault zone architecture and permeability structure. *Geology*, **24**, (1996), 1025-1028.

Clerc, N., Moscariello, A.: A revised structural framework for the Geneva Basin and the neighboring France region as revealed from 2D seismic data: implications for geothermal exploration. *Swiss Bulletin for Applied Geology,* **25**, (2020), 109–131.

Dershowitz, W.S., Herda, H.H.: Interpretation of Fracture Spacing and Intensity, *Rock Mechanics*, (1992), 757–766.

Ferrill, D.A., Smart, K.J., Morris, A.P.: Fault failure modes, deformation mechanisms, dilation tendency, slip tendency, and conduits v. seals, *Geological Society, London, Special Publications*, **496**, (2020), 75–98.

Fleuchaus, P., Godschalk, B., Stober, I., Blum, P.: Worldwide application of aquifer thermal energy storage – A review. *Renewable and Sustainable Energy Reviews,* **94**, (2018), 861–876.

Hauvette, L.: Tectonics of the Western North Alpine Foreland Based on Seismic interpretation of the Greater Geneva Basin, PhD Thesis, *University of Fribourg (Switzerland)*, Fribourg, (2023), 286p.

HGE: GEo-01 Rapport de Fin de Sondage version 1.0. *Report for SIG*, Geneva Switzerland, (2019).

HGE : Conceptualisation géologique, hydrogéologique et thermique du bassin genevois, *Report for SIG*, Geneva, (2021a), 270p.

HGE : Caractérisation des unités réservoirs ("plays stratigraphiques") du Malm supérieur : Modèle lithostratigraphique des horizons productifs potentiels, *Report for SIG*, Geneva, (2021b), 95p.

HGE : Caractérisation des unités réservoirs ("plays stratigraphiques") du Malm inférieur : Modèle lithostratigraphique des horizons productifs potentiels intra Malm, *Report for SIG*, Geneva, (2023a), 116p.

HGE : Modélisation thermo-hydraulique des réservoirs géothermiques du bassin genevois. *Report for SIG*, Geneva, (2023b), 88p.

Koumrouyan, M.: Geomechanical characterisation of geothermal exploration borehole, Msc Thesis, *Centre d'Hydrogéologie et de Géothermie, Université de Neuchâtel*, Neuchâtel, (2019), 93p.

Lo, H.Y.: Discrete fracture network modelling in the Geneva Basin (lower cretaceous carbonates): Implication for geothermal exploration, Msc Thesis, *University of Geneva*, Geneva, (2019), 136p.

Polasek, D.: Kinematic and hydrogeological role of the Jura Mountains' Haute-Chaîne fracture network. Msc Thesis, *University of Geneva*, Geneva, (2020), 247p.

Rickman, R., Mullen, M.J., Petre, J.E., Grieser, W.V., Kundert, D.: A practical use of shale petrophysics for stimulation design optimization: all shale plays are not clones of the barnett shale, *SPE Annual Technical Conference and Exhibition*, Denver, USA, (2008), 11p.

Rusillon, E., 2017. Characterisation and rock typing of deep geothermal reservoirs in the Greater Geneva Basin (Switzerland & France), PhD Thesis, *University of Geneva*, Geneva, (2017), 257p.

Sanderson, D.J., Nixon, C.W.: The use of topology in fracture network characterization, *Journal of Structural Geology*, **72**, (2015), 55–66.

Schori, M.: The Development of the Jura Fold-and-Thrust Belt: pre-existing Basement Structures and the Formation of Ramps, PhD Thesis, *University of Fribourg (Switzerland)*, Fribourg, (2021), 202p.

SFOE: La stratégie énergétique 2050 après l'entrée en vigueur de la nouvelle loi sur l'énergie, *Swiss Federal Office of Energy Publications*, bfe.admin.ch, (2018), 25p.

Terzaghi, R.D.: Sources of Error in Joint Surveys, *Géotechnique*, **15**, (1965), 287–304.

Townend, J., Zoback, M.D.: How faulting keeps the crust strong, *Geology*, **28**, (2000), 399–402.

Zhang, D., Ranjith, P.G., Perera, M.S.A.: The brittleness indices used in rock mechanics and their application in shale hydraulic fracturing: A review. *Journal of Petroleum Science and Engineering*, (2016), 158–170.